University of Glasgow

DEPARTMENT OF

AEROSPACE ENGINEERING

The Estimation Of Helicopter Pilot Workload Using Inverse Simulation - Longitudinal Manoeuvre Analysis

Garry R. Leacock*

Dr. Douglas G. Thomson**

Internal Report No. 9625 October 1996

The Estimation Of Helicopter Pilot Workload Using Inverse Simulation - Longitudinal Manoeuvre Analysis

Garry R. Leacock*
Dr. Douglas G. Thomson**

Internal Report No. 9625 October 1996

*Postgraduate Research Assistant
**Lecturer in Flight Dynamics

Department of Aerospace Engineering
University of Glasgow
Glasgow
G12 8QQ
U.K.

Abstract

In the preceding report the concept of estimating pilot workload using inverse simulation was introduced. The report examined the ADS-33C defined Rapid Side-step Mission Task Element (MTE), and illustrated how various quickness parameters could be obtained from the lateral cyclic pitch and stick displacement time histories. These quickness parameters were plotted on charts and it was shown how the resulting plots could be used to discriminate between two dissimilar helicopter configurations, or identify which manoeuvres were more aggressive and would probably lead to a higher level of workload being placed upon the pilot.

The intention of this report is to provide a supplementary study to the previous one by analysing another linear repositioning manoeuvre, the Rapid Acceleration / Deceleration or Quick-hop MTE. The longitudinal cyclic channel will be investigated in terms of pitch and stick displacement and the equivalent quickness parameters calculated and plotted on charts. A final study mirroring the previous one, on control system influence by the introduction of a Stability and Control Augmentation System, (SCAS) and the alteration of the longitudinal cyclic actuator constant will also be carried out.

Nomenclature

Q_θ pitch attitude quickness parameter

$Q_{\theta 1s}$ longitudinal cyclic pitch quickness parameter

$Q_{\eta 1s}$ longitudinal cyclic stick displacement quickness parameter

t_a time to reach maximum acceleration in Quick-hop Mission Task Element

t_d time to reach maximum deceleration in Quick-hop Mission Task Element

t_m time take to complete entire Quick-hop manoeuvre

V_{max} maximum longitudinal airspeed attained during Quick-hop

$\dot{V}_{max}$ maximum longitudinal acceleration attained during Quick-hop

$\dot{V}_{min}$ maximum longitudinal deceleration attained during Quick-hop

q pitch-rate of helicopter

q_{pk} maximum value of pitch-rate

θ pitch attitude

$\Delta\theta_{min}$ change in pitch attitude corresponding to time taken to attain maximum pitch-rate

θ_{1s} longitudinal cyclic pitch

η_{1s} longitudinal cyclic stick displacement

$I\theta_{1s}$ time integral of longitudinal cyclic pitch

$I\eta_{1s}$ time integral of longitudinal cyclic stick displacement

θ_{1spk} maximum longitudinal cyclic pitch displacement

$\Delta I\theta_{1s}$ change in pitch integral corresponding to time taken to reach maximum longitudinal cyclic pitch displacement

η_{1spk} maximum longitudinal cyclic stick displacement

$\Delta I\eta_{1s}$ stick integral corresponding to time taken to reach maximum longitudinal cyclic stick displacement

1. Introduction

The preceding report described how an initial estimation of pilot workload could be made by calculating certain quickness parameters, and this was illustrated using graphical plots to compare, firstly the workload in three varying aggression Rapid Side-step Mission Task Elements (MTEs) and secondly, two dissimilar helicopter configurations based on the Westland Lynx. It was shown how the lateral cyclic pitch and lateral cyclic stick quickness parameters could be utilised to analyse the control movements of the pilot and the response from the vehicle, as well as highlight the manoeuvre or particular vehicle configuration that demanded a higher percentage of control inputs and hence a greater pilot workload.

The aim of this report is to provide a supplementary study to the previous internal report on pilot workload estimation, using another linear repositioning Mission Task Element, defined along a different axis than the rapid side-step MTE. The Rapid Acceleration / Deceleration MTE or Quick-hop is a manoeuvre performed in much the same way as the rapid side-step but in a longitudinal or 'x-axis' direction and it will again be the Aeronautical Design Standard ADS-33C document, [1] that is the chief source of reference for specifying the manoeuvre parameters.

2. Quick-hop Manoeuvre Definition

ADS-33C documents the key elements of the rapid acceleration / deceleration or quick-hop manoeuvre, Figure 1, as follows:

"Starting from a stabilised hover, initiate a rapid and aggressive longitudinal acceleration up to an airspeed of at least 60 knots, and immediately decelerate to hover over a defined reference point. Maintain a constant altitude at or below 12.1 metres".

Additional desired performance during manoeuvre

- Complete manoeuvre over the reference point at the end of the course. Tolerance is plus zero and minus 3 m (positive forward)
- Maintain heading within ± 10 degrees
- Achieve maximum acceleration in 1.5 seconds or less
- Achieve maximum deceleration within 3.0 seconds of initiating the deceleration phase

2.1 Quick-hop Mathematical Model

It can be seen that there are several similarities between the quick-hop and the side-step and indeed the required times to maximum acceleration and deceleration are identical. However there are two essential differences, firstly the required airspeed is at least 60 knots which is almost twice as fast as the side-step, and secondly the manoeuvre is devoid of a period of zero acceleration, that is, a constant velocity section. The combination of these factors led to the choice of using the manoeuvre mathematical model as developed by Thomson, [2], which consists of three main pulses of longitudinal cyclic, as opposed to four in the side-step. Initially there is a pulse of forward acceleration to pitch the aircraft into the manoeuvre followed by an immediate pulse of deceleration once the required airspeed has been attained. A final pulse of forward longitudinal cyclic is used to bring the aircraft back to a steady trimmed hover state, from the nose up attitude required to decelerate the aircraft.

Figure 2 illustrates the acceleration profile of the quick-hop and it can be seen that the manoeuvre can be broken up in the same manner as the sides-step into a piecewise polynomial, which comprises five distinct and separate elements. The values of $\dot{V}_{max}$ and $\dot{V}_{min}$ are user inputs and to ensure that the ADS performance limits are met, the values of t_a and t_d are set such that,

$$t_a \leq 1.5 \text{ s} \qquad \text{and} \qquad t_d \leq 3.0 \text{ s}$$

Still referring to Figure 2, the third,.fifth and seventh order transient functions covering phases (i) and (v) of the manoeuvre were obtained by the same method as described in the previous report, Section 2.2 and are given in equations 1, 2 and 3 below. The function governing phase (iii) of the manoeuvre was derived in much the same manner.

$$\dot{V}(t) = \left[-2\left(\frac{t}{t_1}\right)^3 + 3\left(\frac{t}{t_1}\right)^2 \right] \dot{V}_{max} \tag{1}$$

$$\dot{V}(t) = \left[6\left(\frac{t}{t_1}\right)^5 - 15\left(\frac{t}{t_1}\right)^4 + 10\left(\frac{t}{t_1}\right)^3 \right] \dot{V}_{max} \tag{2}$$

$$\dot{V}(t) = \left[\frac{10}{3}\left(\frac{t}{t_1}\right)^7 - 14\left(\frac{t}{t_1}\right)^5 + \frac{35}{3}\left(\frac{t}{t_1}\right)^4 \right] \dot{V}_{max} \tag{3}$$

2.1 Quick-hop Manoeuvre Parameters

The quick-hop manoeuvre parameters were chosen to ensure that the maximum amount of longitudinal cyclic was being exploited to perform the manoeuvre without exceeding the control limits while remaining within the required specifications of ADS-33C. As the quick-hop was effectively 'flown' in a different manner than the side-step it was necessary to change some of the manoeuvre parameters, in order to obtain a good spread of points on the subsequent quickness charts. The table below is a summary of the manoeuvre parameters imposed on the three varying aggression quick-hops and it is evident that even the least severe manoeuvre is still a demanding one from a piloting point of view, while the most aggressive manoeuvre is just short of exceeding the control limits.

Quick-hop	V_{max} (kts)	t_a (s)	t_d (s)	$\dot{V}_{max}$, $\dot{V}_{min}$ (m/s^2)
1	60	1.5	3.0	2.0
2	60	1.4	2.8	2.5
3	60	1.3	2.6	3.0

Table 1 Parameters for quick-hop MTEs, least (1) to most aggressive (3)

3. Helicopter Configuration Changes

On conducting the inverse simulation runs it was found that the original Lynx-2 configuration used in the preceding report exceeded the aft longitudinal cyclic pitch limits which invalidated the output data. To ameliorate this problem the decision was taken to improve the vehicle configuration slightly by decreasing the overall mass by 250 kg to 4000 kg, and by increasing the effective rotor stiffness from 50000 Nm/rad to 87500 Nm/rad. The table below summarises the main differences between the two helicopter configurations used in the inverse simulation runs for this report.

Parameter	Lynx-1	Lynx-2
1: Mass (kg)	3500.00	4000.00
2: Blade chord (m)	0.391	0.300
3: C. G. position from reference (m)	0.00	-0.10
4: Equivalent stiffness for centre-spring blade flapping model (Nm/rad)	166352.00	87500.00
5: Height of main rotor above CG (m)	1.271	0.960

Table 2 Configuration data for Lynx-1 and Lynx-2 (improved)

4. The Pitch Attitude Quickness Parameter (Q_θ)

The pitch attitude quickness parameter, Q_θ is calculated using the same formula as that for the roll quickness given in ADS-33C, Section 3.3 and since the inverse simulation package Helinv [3], calculates the time-histories of pitch-rate, q and pitch attitude θ, the pitch attitude quickness can readily be obtained from,

$$\text{Pitch Attitude Quickness, } Q_\theta = \frac{q_{pk}}{\Delta\theta_{min}} \qquad (4)$$

The objective of this section of the report is to draw comparisons between inverse simulation runs conducted using:

a. three varying aggression quick-hop MTEs summarised in Table 1, using the same helicopter configuration and,

b. two dissimilar helicopter configurations based on the Westland Lynx, simulated using the same quick-hop Mission Task Element.

4.1 Comparison of Pitch Attitude Quickness for Varying Aggression Quick-hop MTEs

Severity of the quick-hops was varied by gradually decreasing the time taken to reach maximum acceleration, (t_a) and deceleration, (t_d) and also by increasing the value of the maximum acceleration, deceleration, ($\dot{V}_{max}$ and $\dot{V}_{min}$). The pitch attitude time-histories for the three quick-hops are presented in Figures 3a through c, with the three main pulses of longitudinal cyclic being evident. It can also be seen that the maximum pitch-rate, q_{pk} does not increase greatly as the manoeuvre becomes more aggressive and this is confirmed by the quickness chart, Figure 4 which shows only a gradual increase in quickness. Note that the points on Figure 4 move upwards and to-the-right as aggression is increased; the decrease in time to maximum acceleration, deceleration being responsible for the upwards movement with

the actual value of the maximum acceleration, deceleration being accountable for the movement to-the-right. Another trend that is evident in Figure 4 is that the points are clumped together, either in pairs or as single values. The paired points are representative of the initial pulse of acceleration to pitch the aircraft into the manoeuvre and the final pulse of acceleration to restore the aircraft to its' original trim position, while the single points closer to the bottom of the figure are illustrative of the deceleration pulse in the middle of the manoeuvre to reduce the aircraft's speed towards zero.

3.2 Comparison of Pitch Attitude Quickness For Two Dissimilar Lynx Configurations

Quick-hop number two was chosen as the test case for two different Lynx configurations. The time-histories of pitch-rate and pitch attitude for the simulation runs are shown in Figures 5a and b and it is obvious that the maximum pitch-rate is very similar for each aircraft at about 23 or 24 deg/s. The main noticeable difference that discriminates one aircraft from the other is the larger oscillations following the pulses of longitudinal cyclic, and it will be shown in later sections of the report how this has a negative contribution to pilot workload.

On plotting the resulting quickness chart, Figure 6, the same conclusion can be drawn as in the previous report, Section 3.2; that is, the pitch attitude quickness is dependant specifically on the manoeuvre profile itself, and since both runs were conducted using the same quick-hop MTE it follows that the resulting quickness values are of a similar nature. This result is typical of many others obtained from inverse simulation runs at Glasgow University and it has been generally accepted that the quickness chart values obtained for dissimilar helicopter configurations will be comparable unless gross changes are made to one vehicle, in which case the helicopter is unlikely to be able to 'fly' the manoeuvre as control limits will probably be exceeded.

Pitch attitude quickness although useful, cannot be directly used for pilot workload estimation, but is more a tool of performance comparison. However, the charts in Figures 4 and 6 do show that not all of the points lie in the Level 1 region, [4], and this in itself is an indication as to the level of flying quality achieved during that portion of the manoeuvre. It can be seen that for both vehicles and all three quick-hops the middle pulse of longitudinal cyclic to decelerate the aircraft, produces quickness values that are in the Level 2 region which is an area of slightly degraded handling qualities. To get a better indication of pilot workload however, it is necessary to introduce another parameter, the longitudinal cyclic pitch quickness parameter, $Q_{\theta 1s}$, which will be discussed in more detail in the following section.

5. The Longitudinal Cyclic Pitch Quickness Parameter ($Q_{\theta 1s}$)

Calculated in exactly the same manner as the lateral cyclic pitch quickness the longitudinal pitch attitude quickness takes the peak value of longitudinal cyclic and divides it by the corresponding integral of change in attitude, and is given mathematically as,

$$\text{Longitudinal cyclic pitch quickness } (Q_{\theta 1s}) = \frac{\theta_{1spk}}{\Delta I\theta_{1s}} \qquad (5)$$

where I represents the time integral of the longitudinal cyclic.

This is a method which can be used to assess the pilot workload situation in a given manoeuvre and is extremely useful in manoeuvre or vehicle comparison as control limits can be superimposed on the quickness charts to give an indication of the amount of available longitudinal pitch.

4.1 Comparison of Longitudinal Cyclic Pitch Quickness for Varying Aggression Quick-hop MTEs

The time-histories of longitudinal cyclic pitch and its' time integral are presented in Figures 7a through c. It can be seen that as the manoeuvre severity increases the pulses of cyclic pitch increase correspondingly with the most aggressive quick-hop producing values that are almost double that of the more gentle manoeuvre. On viewing the longitudinal cyclic pitch quickness chart, Figure 8, it is again possible to observe the upward and to-the-right trend of the initial and final acceleration pulses. The middle pulses of deceleration do not seem however, to produce a trend that is immediately discernible, although on closer inspection it is possible to speculate that these pulses are following a hyperbolic trend, that is, as the manoeuvre becomes more aggressive the quickness amplitude increases and the time integral of the corresponding change in longitudinal cyclic pitch becomes less. Figure 8 is annotated with hyperbolic contour lines representing 100% and 50% of the cyclic pitch limit available.

4.2 Comparison of Longitudinal Cyclic Pitch Quickness For Two Dissimilar Lynx Configurations

The longitudinal cyclic pitch quickness chart presented in Figure 10 was produced using the time-histories in Figures 9 a and b. It can be seen that it is an excellent tool for discriminating between the two helicopters, as it unambiguously identifies Lynx-2 as being an inferior helicopter since larger control inputs are required to perform the same manoeuvre. This is illustrated on the chart simply by the fact that the quickness value points for Lynx-2 approach the 100% contour more closely than those of Lynx-1, suggesting that a higher percentage of the maximum lateral cyclic control is being used.

Figure 11 shows all three quick-hop results for each Lynx and although the chart initially seems cluttered with points, it is still possible to identify the points of acceleration

which occur in pairs for each configuration, and the middle pulses of deceleration which follow the hyperbolic trend. For each configuration the quickness values are similar but it is Lynx-2 that produces values that are pushed towards the right of the chart near the control limits, suggesting that greater control movements are required to perform the same manoeuvre hence producing a higher workload for the pilot. The cyclic pitch frequency chart, Figure 12 also shows that Lynx-2 has a higher frequency of larger control inputs and is therefore more likely to meet physical control limits which would retard the performance ability of the vehicle, while imposing a higher workload penalty on the pilot.

6. The Longitudinal Cyclic Stick Displacement Quickness Parameter ($Q_{\eta 1s}$)

The longitudinal stick quickness parameter is perhaps a more useful tool for analysing the pilot workload as it permits the actual stick movements of the pilot to be analysed. Helinv produces the time-histories for longitudinal cyclic stick displacement and it is a simple matter to integrate them and obtain the quickness from the equation,

$$\text{Longitudinal cyclic stick quickness } (Q_{\eta 1s}) = \frac{\eta_{1spk}}{\Delta I\eta_{1s}} \qquad (6)$$

where I represents the time integral of the stick position.

6.1 Comparison of Longitudinal Cyclic Stick Quickness for Varying Aggression Quick-hop MTEs

The results obtained from the comparison of the three quick-hop MTEs confirm those obtained in the previous section, and identify quick-hop three as being the most severe and difficult to fly, with some pulses on the time-histories, illustrated in Figures 13a, b and c, requiring twice as much stick displacement than the first quick-hop. These results filter

through to the quickness chart in Figure 14, where it is quick-hop three that produces values closer to the available limit, annotated by the 100% contour line.

6.2 Comparison of Longitudinal Cyclic Stick Quickness For Two Dissimilar Lynx Configurations

Further evidence of degraded handling qualities and higher pilot workload in the inferior Lynx-2 configuration are evident in the time-histories in Figures 15a and b, and in the quickness chart in Figure 16 which show the vehicle to have higher percentages of stick displacements and quickness values closer to the available longitudinal cyclic stick control limit. Once again the points of acceleration appear in pairs, although it is not really possible to identify a hyperbolic trend in the two points of deceleration. Another influencing factor on pilot workload is the amount of overshoot after an initial stick displacement. It can be seen that Lynx-2 requires more compensatory overshoot requiring the pilot to work harder and complicating an otherwise simple manoeuvre.

Figure 17 presents the longitudinal cyclic stick quickness chart for both Lynx configurations simulated over all three quick-hops, resulting in a total of 18 quickness values. Once again it is possible to identify the points of acceleration for each aircraft and manoeuvre and the hyperbolic trend in the points of deceleration. The fact that Lynx-2 uses more of the available control than Lynx-1 is illustrated and more readily understood in the longitudinal cyclic stick displacement frequency chart, Figure 18, where the peak displacements are shown as percentages of the total stick used to perform the manoeuvres.

7. Preliminary Study On Control System Interference

In keeping with the study performed in the previous report, an initial investigation was carried out into the effects of firstly introducing a Stability and Control Augmentation System to the inverse simulation runs, and secondly looking at the consequences of altering the value of the longitudinal cyclic actuator time constant, τ_{c1}. Two test cases were simulated; setting the time constant to zero, that is, in effect having instantaneous pitch motion after a stick input, and setting τ_{c1} to twice its' normal value at 0.25. A more comprehensive study of the longitudinal cyclic channel is given in Appendix A.

7.1 Effect of Using a Stability and Control Augmentation System During Quick-hop MTE

The previous conclusion drawn from the investigation into the effect of using a SCAS during the side-step was that pilot workload was reduced considerably. On observing Figures 19a and b, it is evident that the SCAS does not have such a large influence on the longitudinal behaviour of the cyclic stick, as the two time-histories are virtually identical. However, it is evident from the quickness chart in Figure 20, that there is a slightly beneficial effect, but only just, as the scale of the chart illustrates. The quickness values for each test case are very similar and it is only the drift of points to the right in the case of the normal Lynx that discriminates it as being inferior to utilising the SCAS during the manoeuvre.

7.2 Effect of Setting the Longitudinal Actuator Time Constant to Zero (τ_{c1}=0.0)

The longitudinal actuator time constant is a pure time delay taken for the control input of the pilot to have effect on the rotors, resulting in a pitch change and a forward or rearward tilt of the rotor disc. A typical value of τ_{c1} for the Westland Lynx helicopter is around 0.125

seconds, and it is therefore expected that reducing this value to zero will have a beneficial effect on the workload imposed on the pilot. Figure 21b shows the cyclic stick time-history for the zero τ_{c1} setting, and it can be seen that the required control inputs are not as large compared to the normal case, Figure 21a. This is better represented on the quickness chart in Figure 22 as the instantaneous actuator produces the most favourable results in terms of pilot workload, being further away from the control limit contour.

7.3 Effect of Doubling the Longitudinal Actuator Time Constant to Zero (τ_{c1}=0.25)

Figure 21c illustrates the point that the required control movements are greater for the increased actuator constant time setting, and this is confirmed on the quickness chart, Figure 22 as the points are located closer to the available control limit. This suggests that if the actuator time constant were increased still further, the control limits would be reached and this vehicle configuration would be incapable of 'flying' the manoeuvre.

8. Conclusions

The work in this report was aimed at providing a supplementary study to the preceding one, Internal Report number 9624, which conducted a similar investigation into lateral cyclic using the Rapid Side-step MTE. The main aspect of this report was centred on the analysis of pilot workload and the longitudinal cyclic channel using the Rapid Acceleration / Deceleration or Quick-hop Mission Task Element.

The mathematical model used to drive the simulations in this report was different to the preceding one, in that it consisted of three pulses of cyclic as opposed to four, but was more suited to the definition of the manoeuvre as given by ADS-33C, as it neglected to include the

period of zero acceleration in the middle of the manoeuvre. Studies were conducted firstly on three quick-hops of varying aggression and secondly on the comparison of workload between two dissimilar helicopter configurations based on the Westland Lynx. It was again shown how the cyclic pitch quickness parameter could be used to identify a manoeuvre, or portion of a manoeuvre which would pose the greatest problems for a pilot. The ability to discriminate unambiguously between the two helicopters was also a distinct advantage of the quickness parameter, and it was illustrated how it could be used for this purpose.

A new parameter introduced in the last report was also utilised in this report, the cyclic stick quickness parameter, and was subsequently used to analyse the longitudinal channel of the vehicles and manoeuvres under consideration. This was shown to have conceivably more potential in pilot workload analysis, and of equal importance confirmed the results obtained using the cyclic pitch quickness parameter. One method of commenting on pilot workload that was mentioned briefly, was that more aggressive manoeuvres and inferior helicopter configurations tended to produce so called control overshoots in the resulting time histories, and a suggestion for further study could be made at this point.

The final study to be conducted in this report was the analysis of cyclic stick time-histories when, firstly, a SCAS was activated and secondly the value of the longitudinal actuator constant was altered. The results obtained mirror those in the previous report and suggest generally that a SCAS can considerably improve the workload situation in the cockpit, while the reduction of the value of the cyclic actuator time constant also produces favourable effects on the subsequent results.

It can be concluded then, that the utilisation of quickness parameters can be used for the study of pilot workload and to a certain extent handling qualities, and can be modified and adjusted to suit the needs of the user and the manoeuvre that is being analysed.

References

1. Anon., "Aeronautical Design Standard, Handling Qualities Requirements for Military Rotorcraft." ADS-33C, August 1989.

2. Thomson, D. G., Bradley, R., "The Contribution of Inverse Simulation to the Assessment of Helicopter Handling Qualities." Paper 7.3.2, Proceedings of the 19th ICAS Conference, Anaheim USA, September 1994.

3. Thomson, D. G., Bradley, R., "Development and Verification of an Algorithm for Helicopter Inverse Simulation." Vertica, Vol. 14, No. 2, May 1990.

4. Cooper, G. E., Harper, Jr., R. P. "The Use of Pilot Rating in the Evaluation of Aircraft Handling Qualities." NASA TN D-5153.

5. Thomson, D. G., Bradley, R., "Mathematical Definition of Helicopter Manoeuvres." Department of Aerospace Engineering, University of Glasgow, Internal Report No. 9225, June 1992.

Appendix A

The Longitudinal Cyclic Channel

Like the lateral cyclic channel, longitudinal cyclic is applied through the swashplate and is used to direct the thrust vector either forwards or backwards pitching the aircraft about its' centre of gravity resulting in longitudinal motion.

In the aircraft's Automatic Flight Control System (AFCS), the pilot contribution to longitudinal cyclic displacement prior to cyclic mixing is actually derived from a combination of longitudinal cyclic and collective lever positions, and the relationship between them can be seen in the following equation:

$$\theta_{1sp}^{*} = g_{1s0} + g_{1s1}\,\eta_{1s} + (g_{sco} + g_{sc1}\,\eta_{1s})\,\eta_{c}$$

where,

θ_{1sp}^{*} is the pilot contribution to longitudinal cyclic displacement before mixing,

g_{1s0} and g_{1s1} are longitudinal cyclic stick gearing constants,

g_{1c0} and g_{1c1} are collective lever gearing constants,

η_c is the collective lever position ($0 \leq \eta_c \leq 1$) and

η_{1s} is the longitudinal cyclic stick displacement ($0 \leq \eta_{1s} \leq 1$)

The SCAS contribution to the longitudinal cyclic channel is obtained via feedback from the pitch-rate, q and pitch attitude, θ of the helicopter. An additional feed-forward term based on the position of the cyclic stick and current trim position is also included to permit enhanced vehicle response to a given longitudinal cyclic stick input.

Therefore the lateral cyclic contribution from the SCAS, θ_{1sa}^{*} is obtained from:

$$\theta_{1sa}^{*} = k_{\theta}\theta + k_{q}\, q + k_{1s}\,(\eta_{1s} - \eta_{1s0})$$

where,

k_{θ} is a proportional action feedback gain,

k_{q} is a derivative action feedback gain,

k_{1s} is the feed-forward gain and

η_{1s0} is the reference pilot stick position, $(0 \leq \eta_{1s0} \leq 1)$

The transfer function of the combined pilot and SCAS is given by:

$$\frac{\theta_{1s}^{*}}{\theta_{1sp}^{*} + \theta_{1sa}^{*}} = \frac{1}{1 + \tau_{c1}\, s}$$

where τ_{c1} is the lateral cyclic actuator time constant

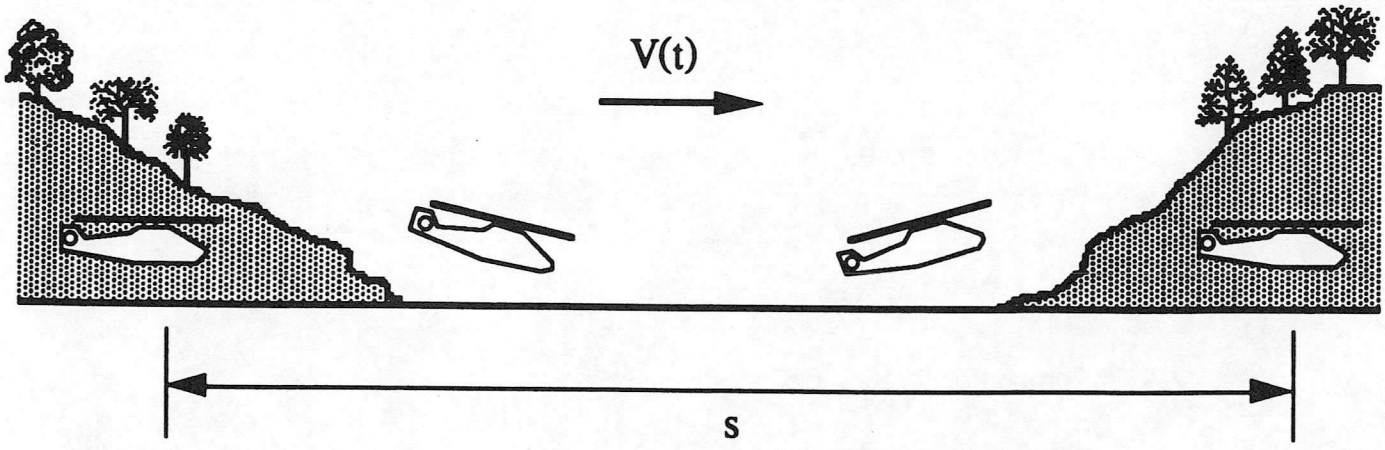

Figure 1 **Illustration of Rapid Acceleration / Deceleration (Quick-hop) Mission Task Element (MTE), [5]**

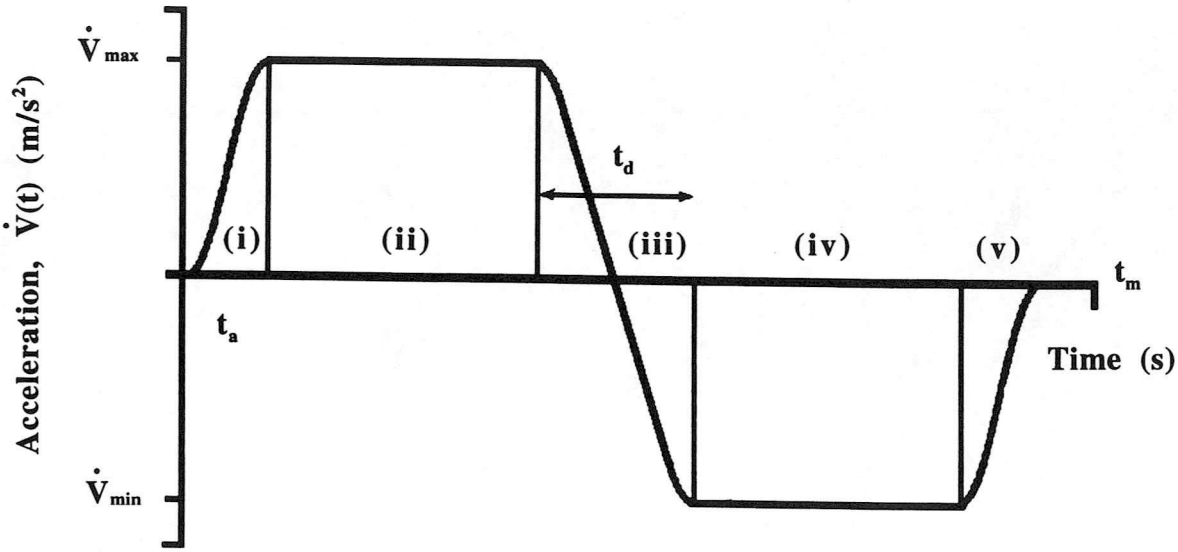

Figure 2 Acceleration profile of Quick-hop

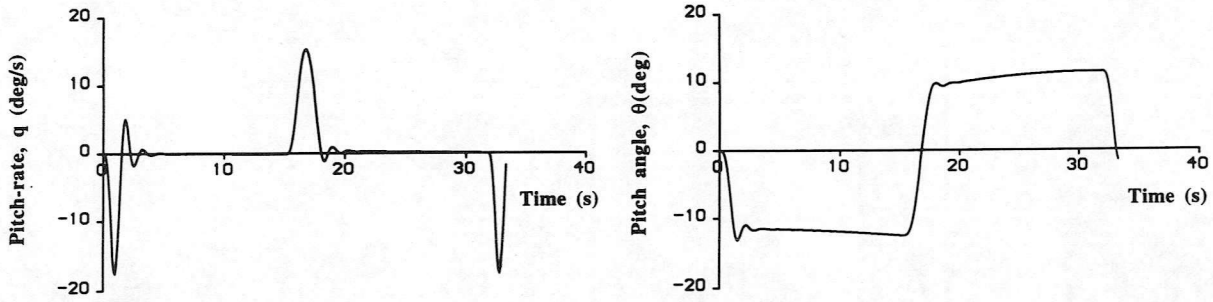

(a) Quick-hop 1

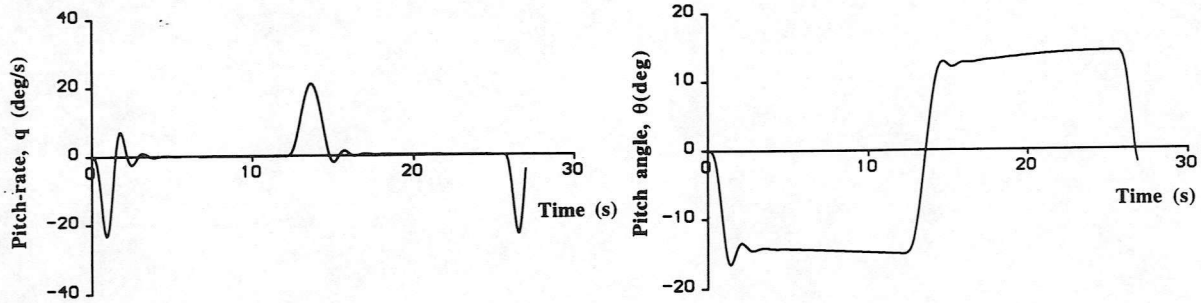

(b) Quick-hop 2

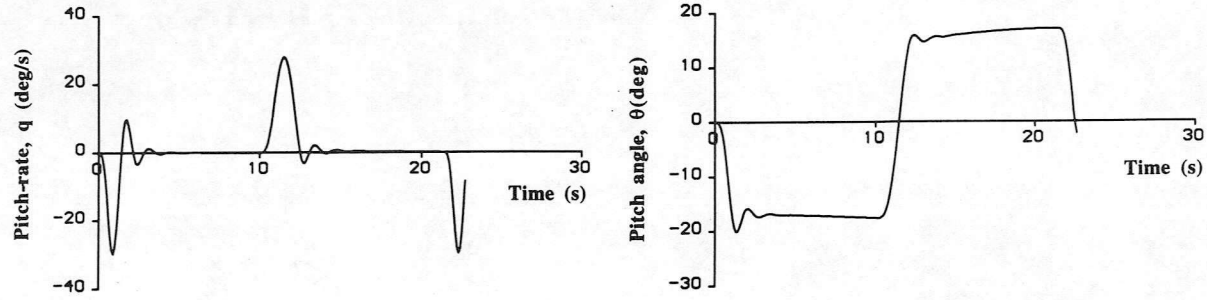

(c) Quick-hop 3

Figure 3 **Pitch-rate, q and roll angle, θ time-histories for three Quick-hop MTEs**

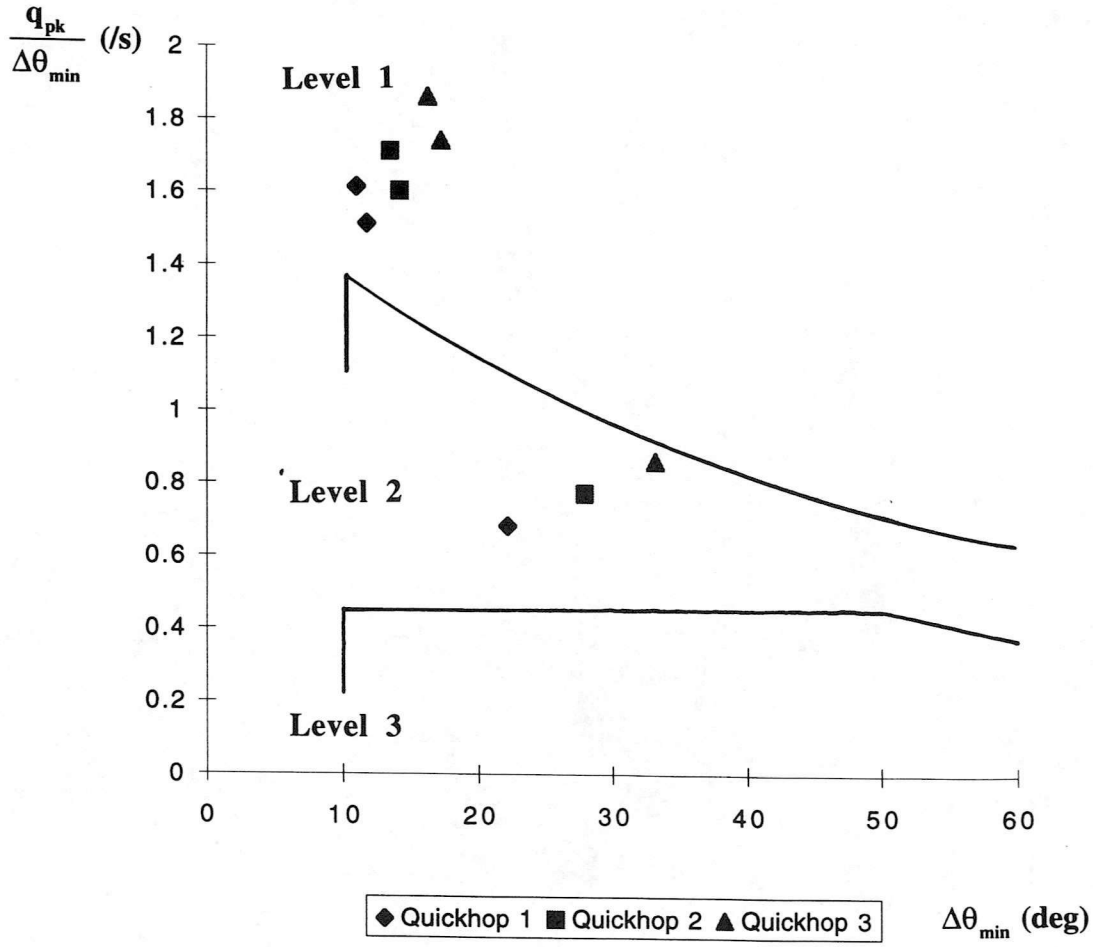

Figure 4 **Pitch Attitude quickness chart calculated using Figure 3 time-histories**

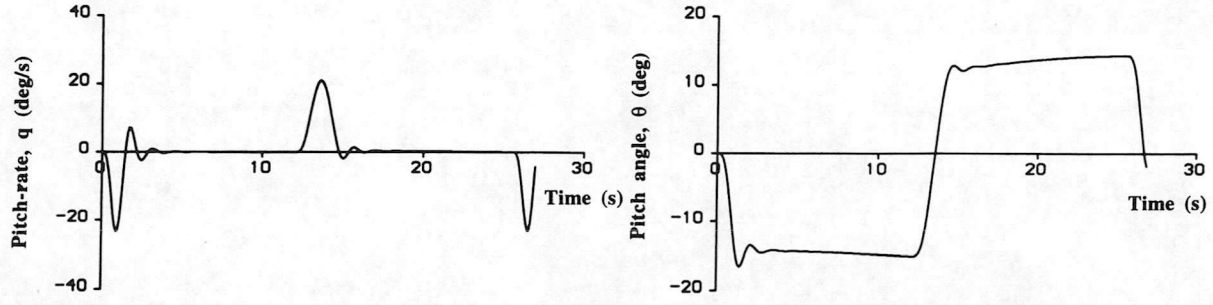

(a) Lynx-1

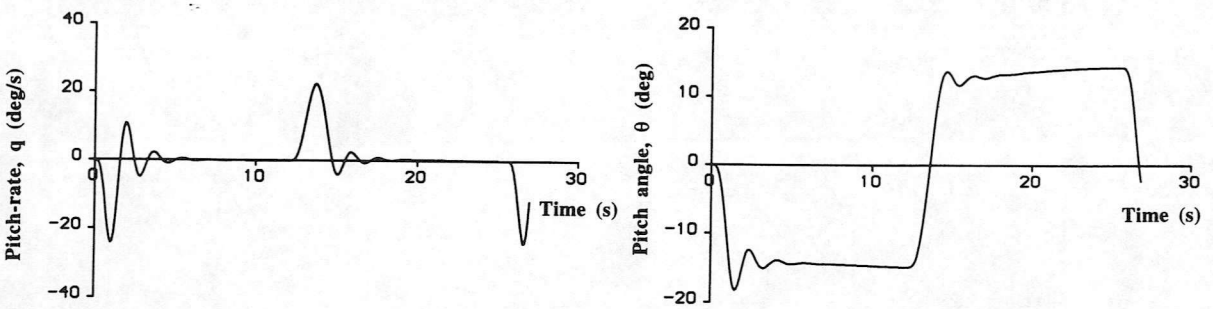

(b) Lynx-2

Figure 5 Pitch-rate, q and roll angle, θ time-histories for the two dissimilar Lynx configurations

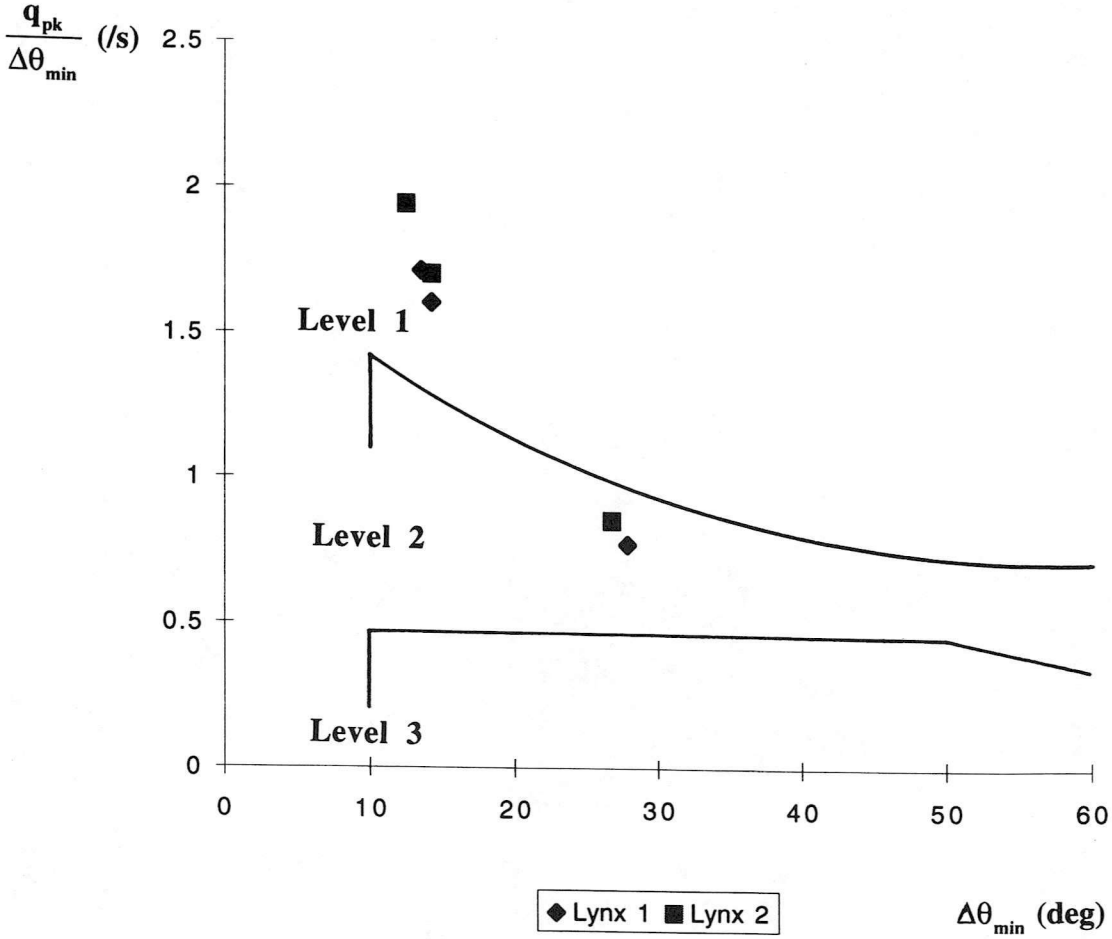

Figure 6 **Pitch Attitude quickness chart calculated from Figure 5 time-histories**

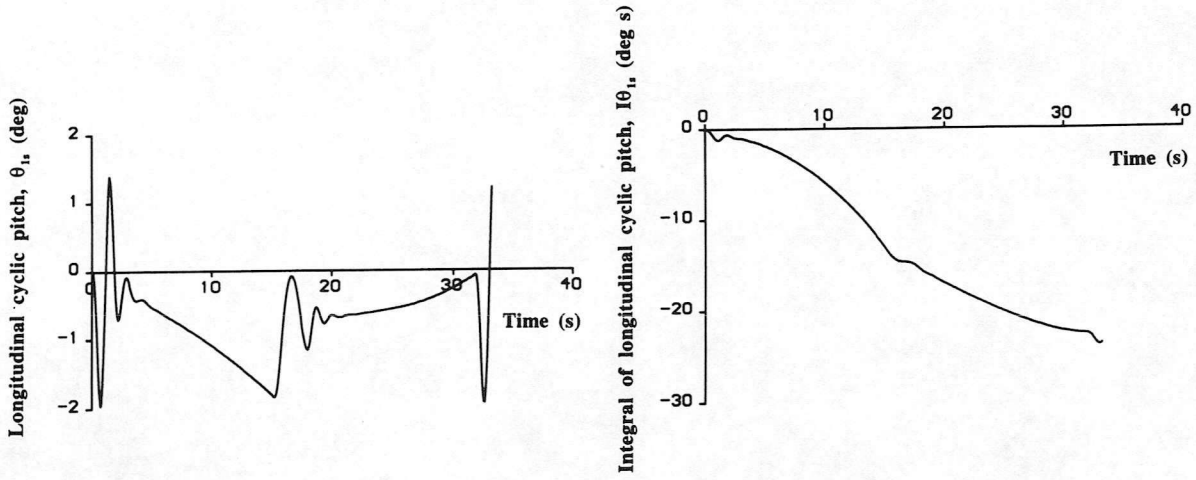

(a) Quick-hop 1

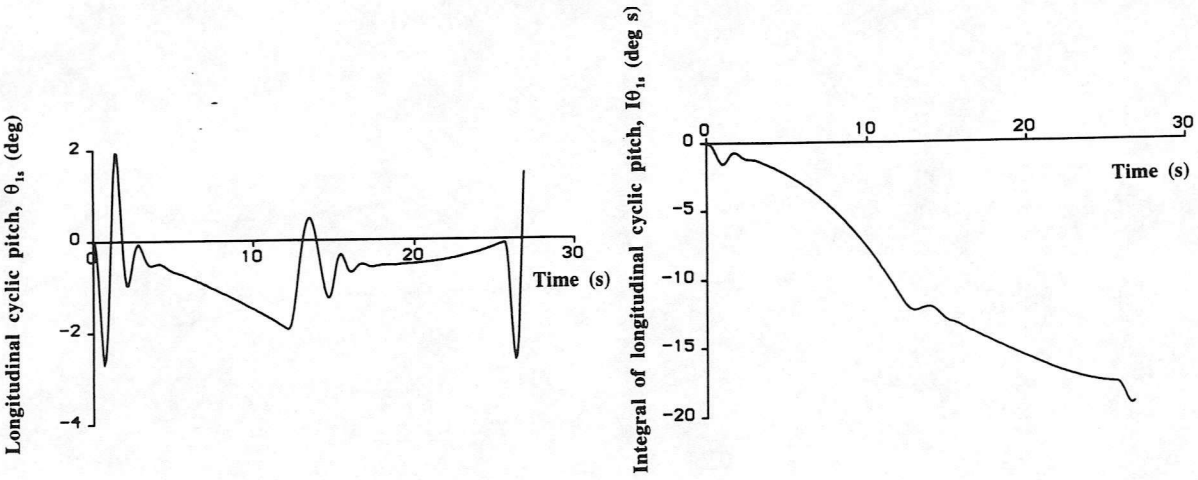

(b) Quick-hop 2

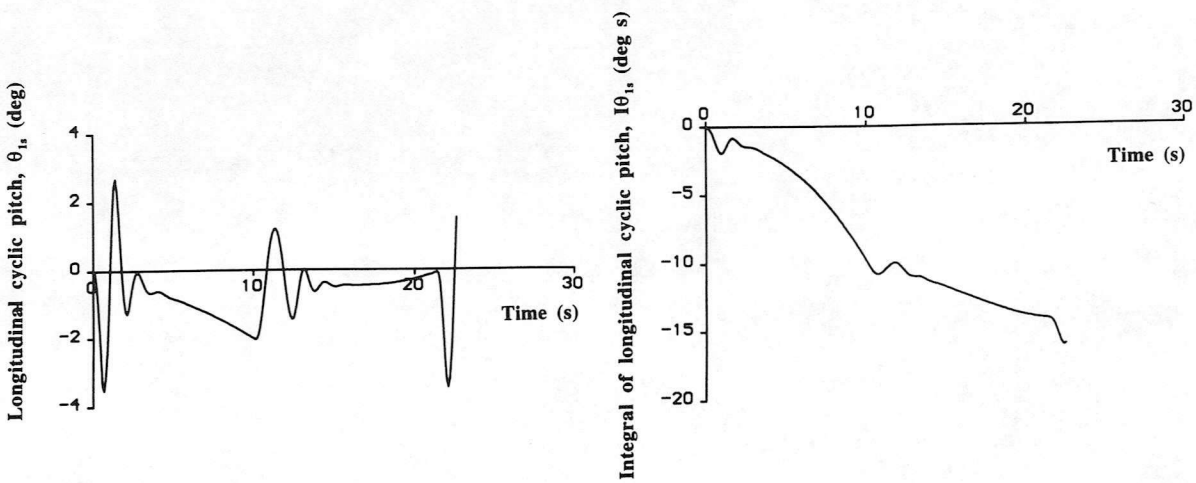

(c) Quick-hop 3

Figure 7 Longitudinal cyclic pitch, θ_{1s} and integral of longitudinal cyclic pitch, $I\theta_{1s}$ time-histories for the three Quick-hop MTEs

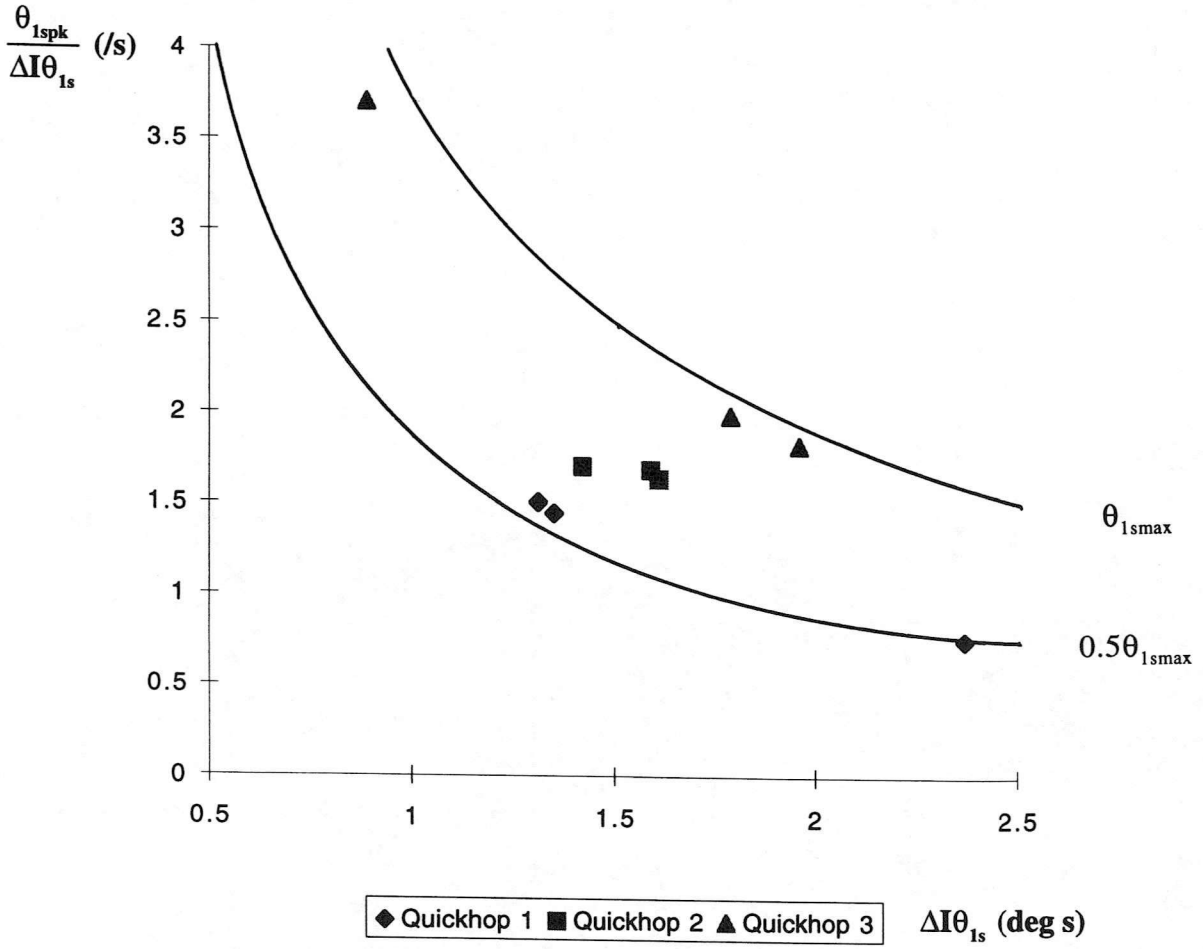

Figure 8 **Longitudinal cyclic pitch quickness chart calculated from Figure 7 time-histories**

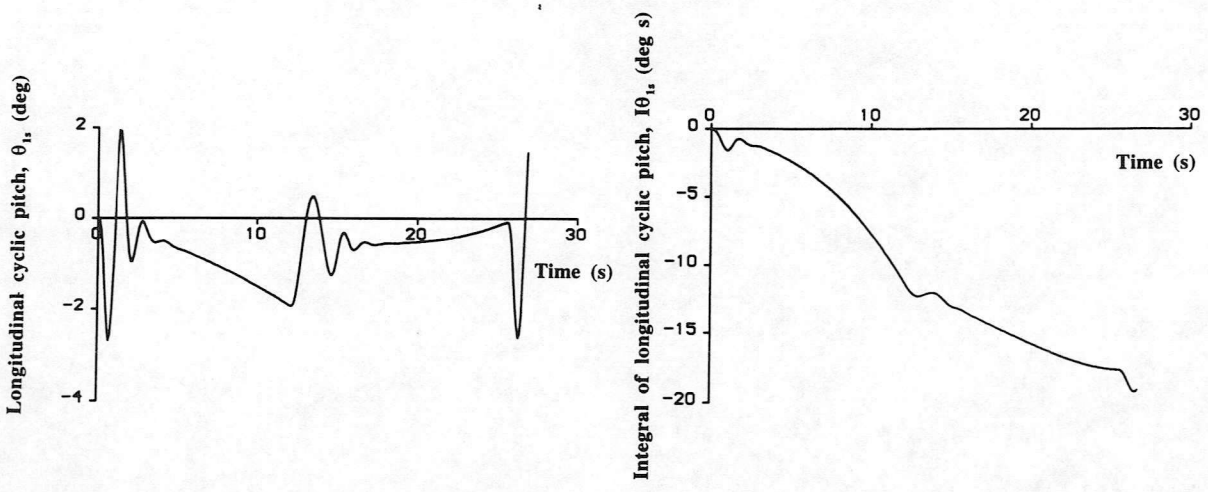

(a) Lynx-1

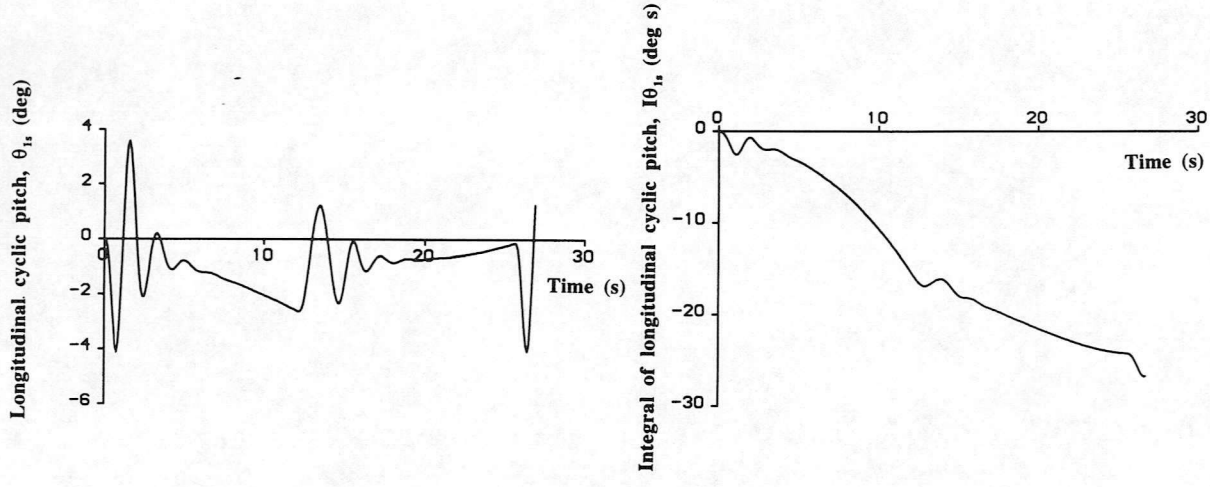

(b) Lynx-2

Figure 9 Longitudinal cyclic pitch, θ_{1s} and integral of longitudinal cyclic pitch, $I\theta_{1s}$ for the two dissimilar Lynx configurations

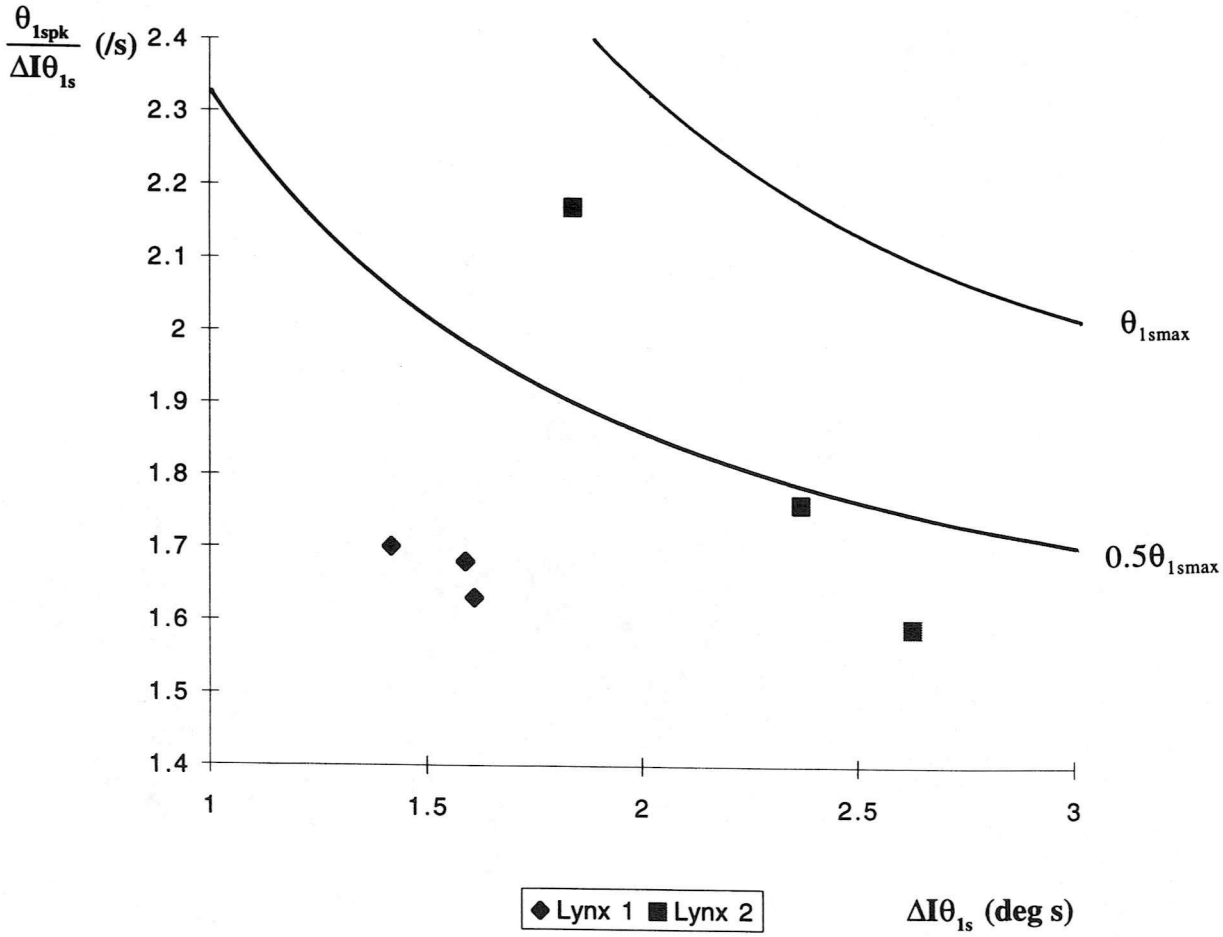

Figure 10 Longitudinal cyclic pitch quickness chart calculated from Figure 9 time-histories

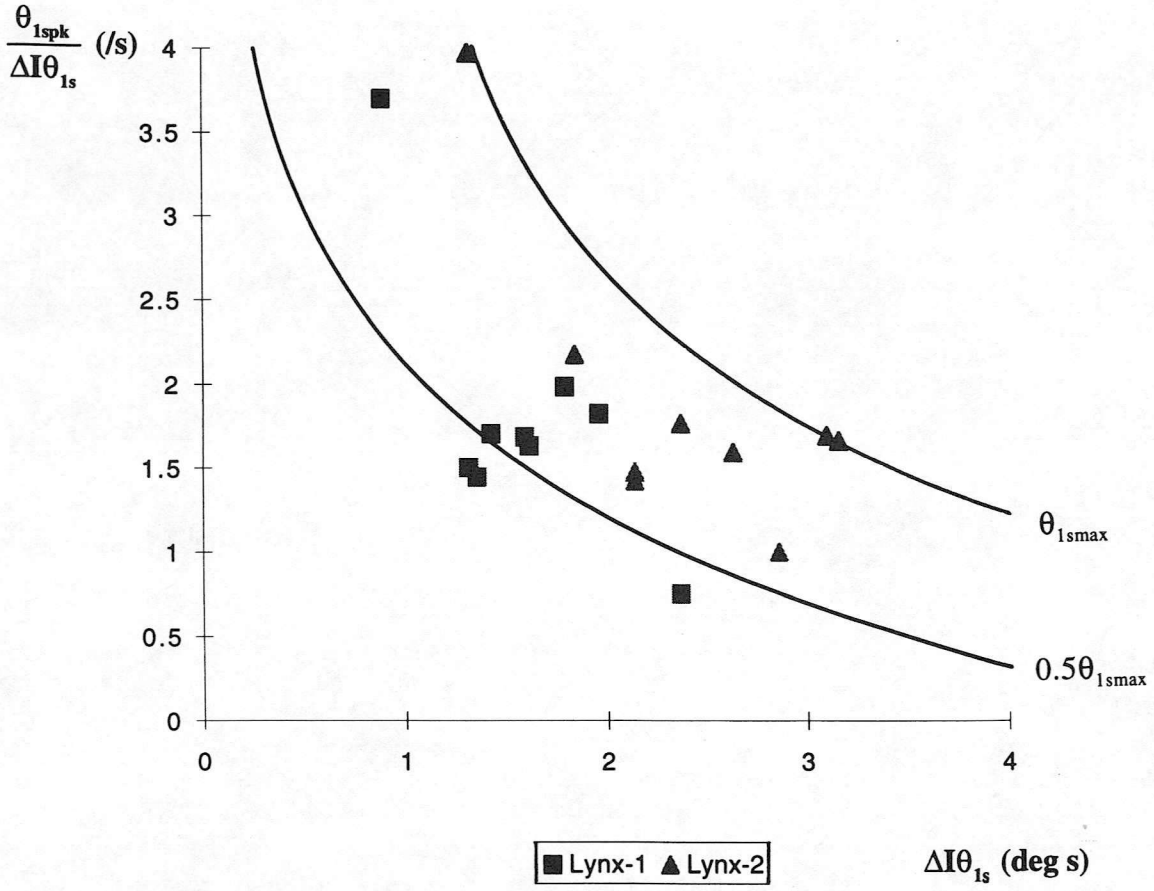

Figure 11 **Longitudinal cyclic pitch quickness chart for both Lynx configurations and all three Quick-hop MTEs**

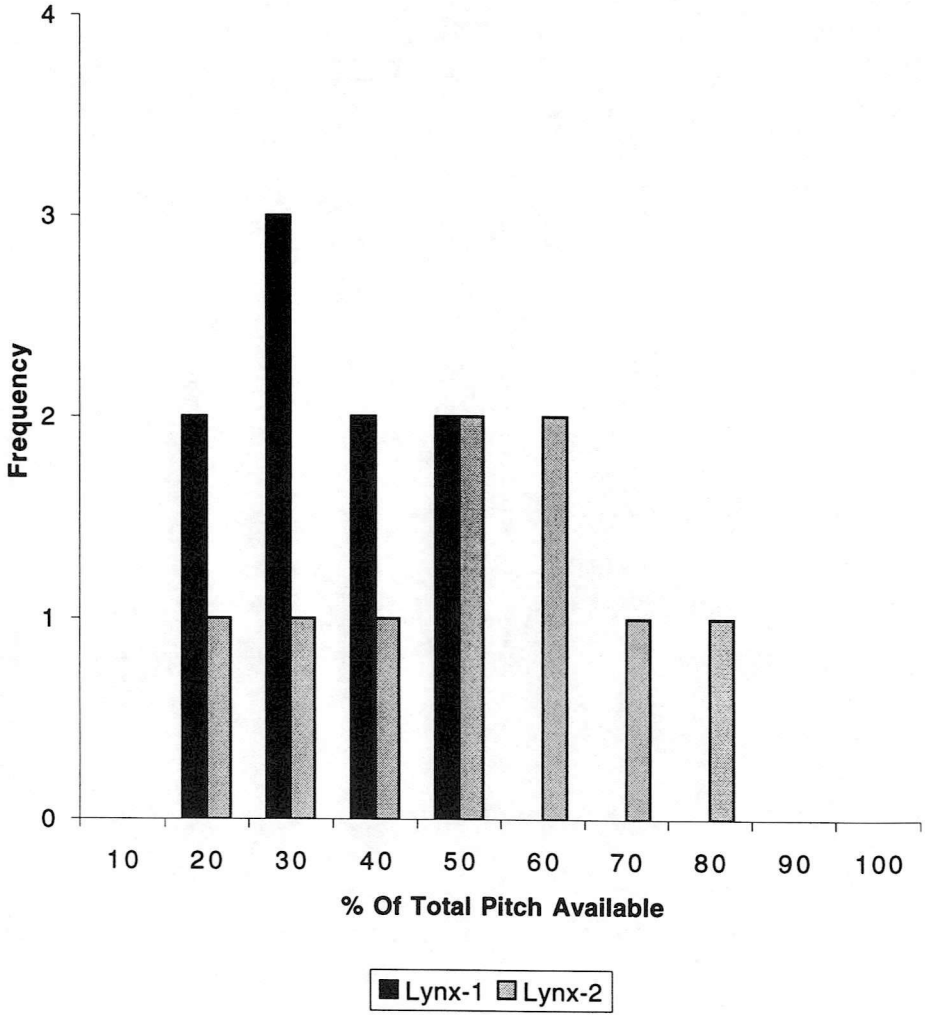

Figure 12 Longitudinal cyclic pitch frequency chart

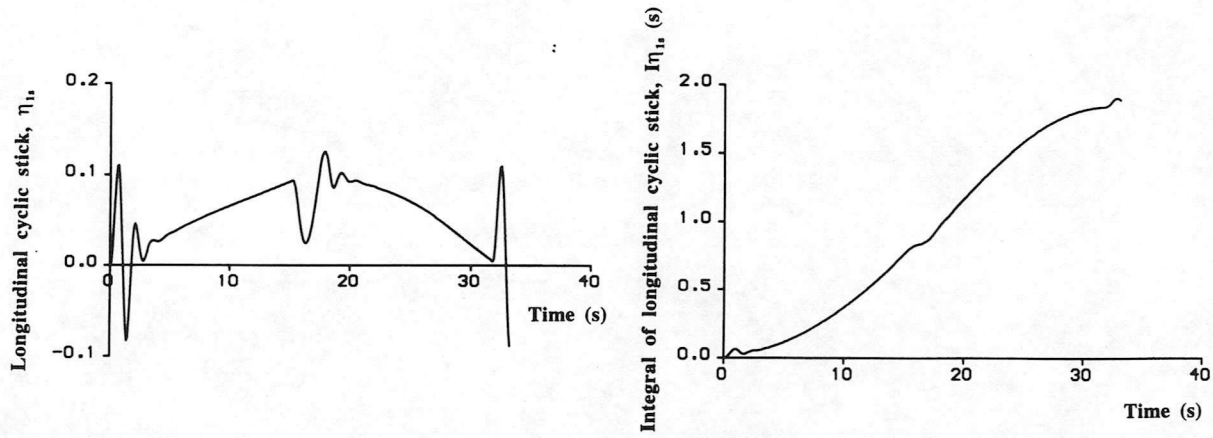

(a) Quick-hop 1

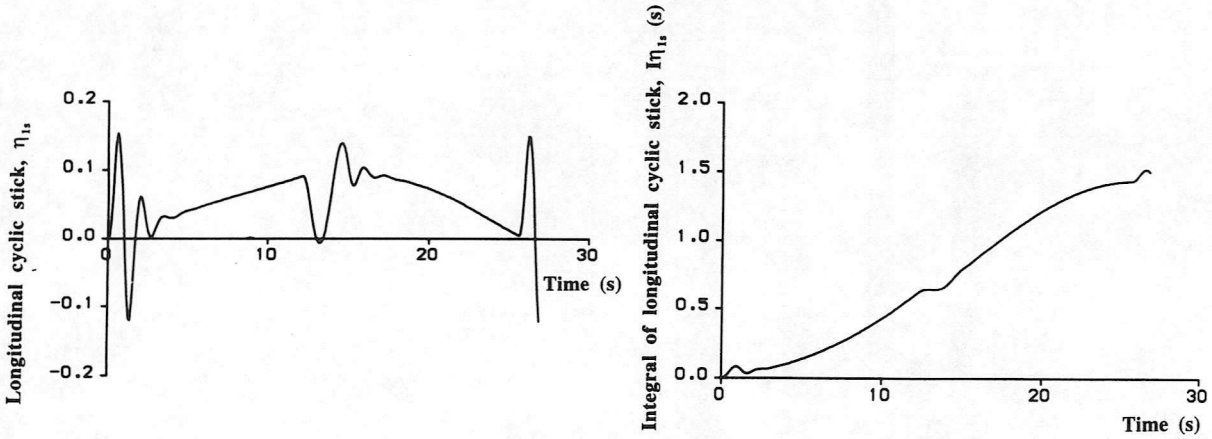

(b) Quick-hop 2

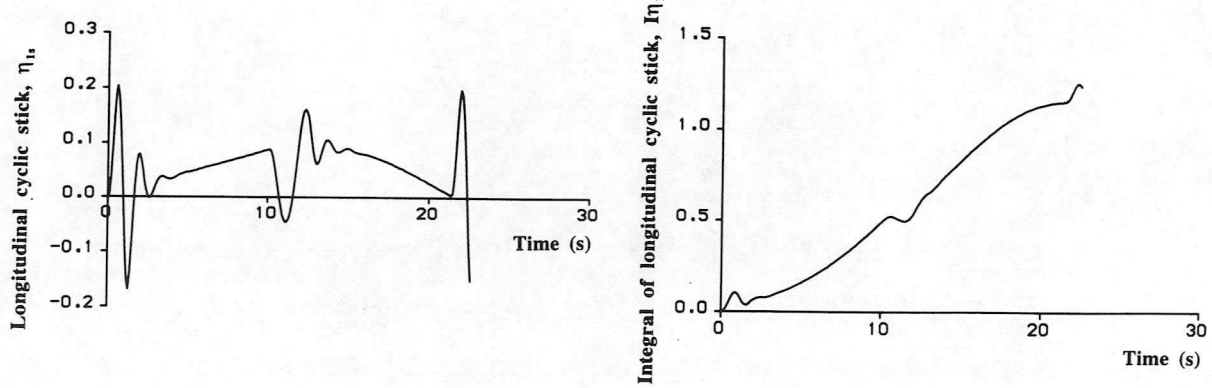

(c) Quick-hop 3

Figure 13 Longitudinal cyclic stick displacement, η_{1s} and integral of longitudinal cyclic stick, $I\eta_{1s}$ time-histories for the three Quick-hop MTEs

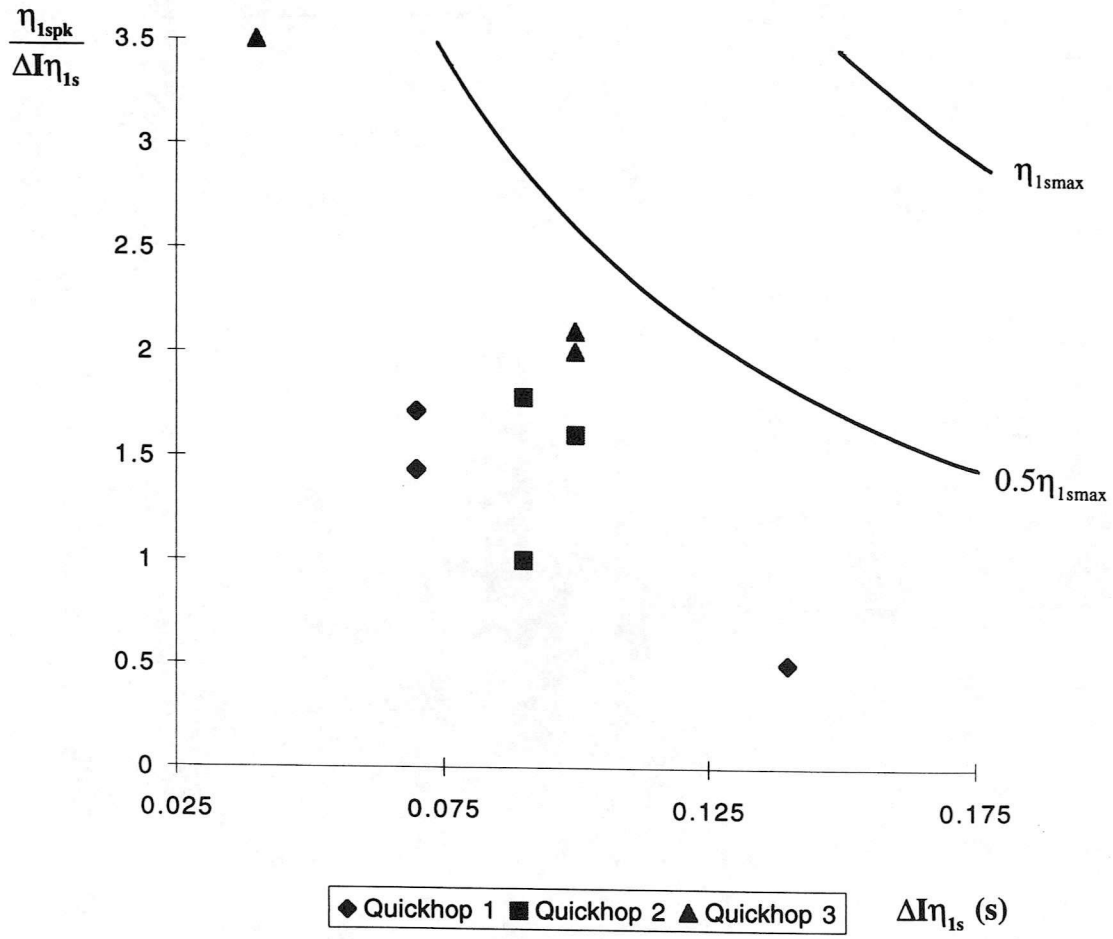

Figure 14 Longitudinal cyclic stick displacement quickness chart calculated from Figure 13 time-histories

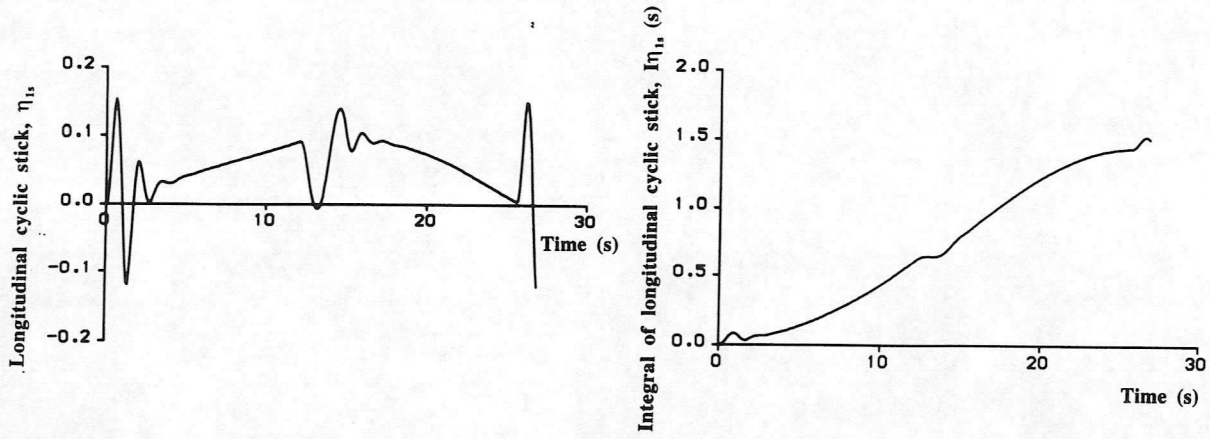

(a) Lynx-1

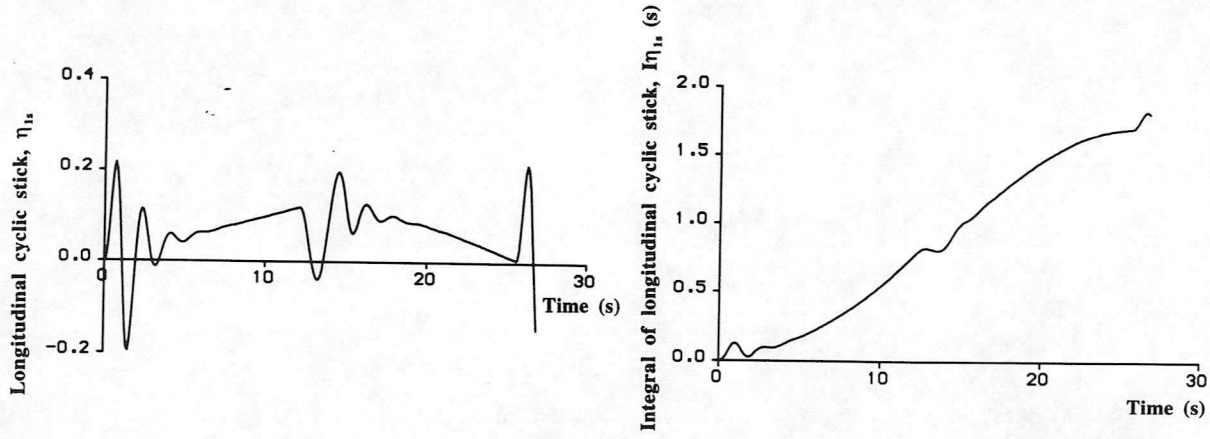

(b) Lynx-2

Figure 15 Longitudinal cyclic stick, η_{1s} and integral of longitudinal cyclic stick, $I\eta_{1s}$ time-histories for the two dissimilar Lynx configurations

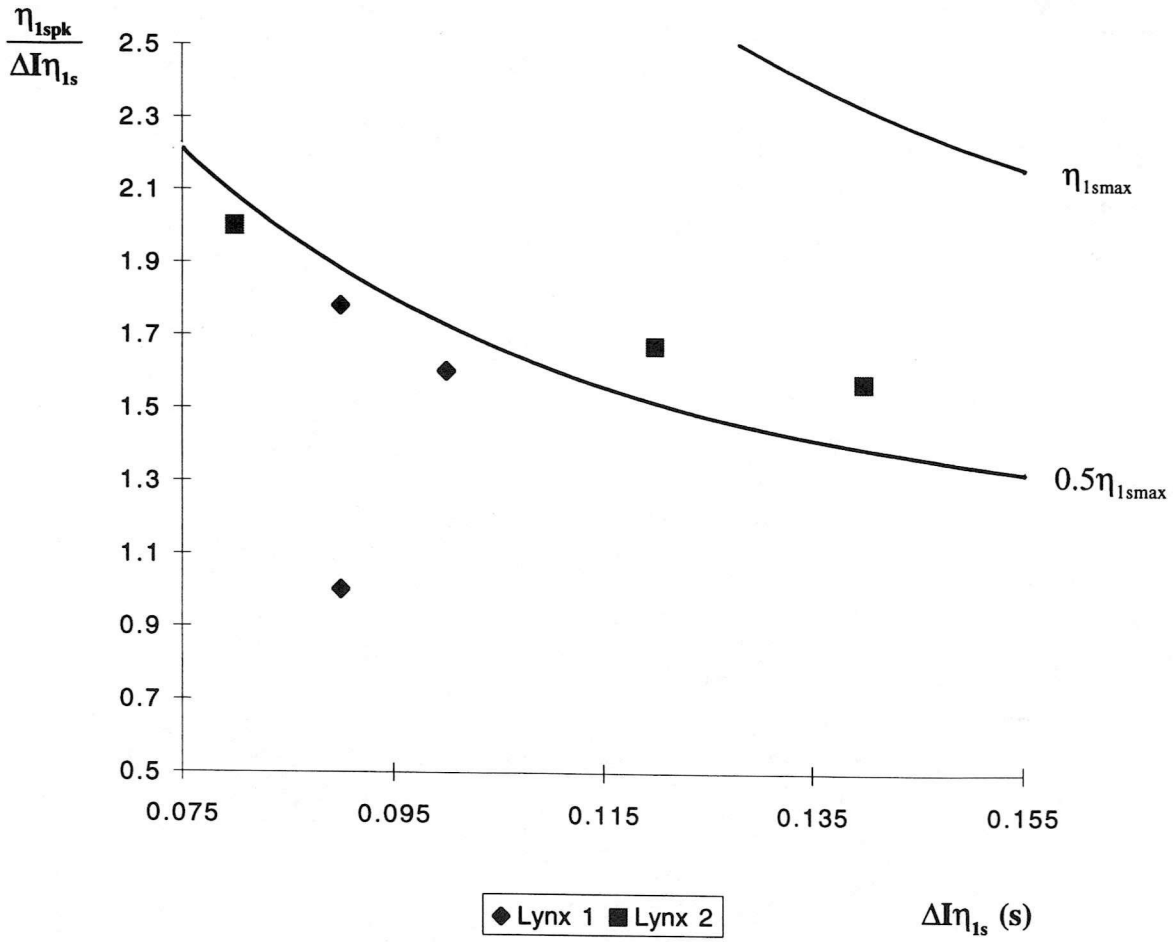

Figure 16 Longitudinal cyclic stick quickness chart calculated from Figure 15 time-histories

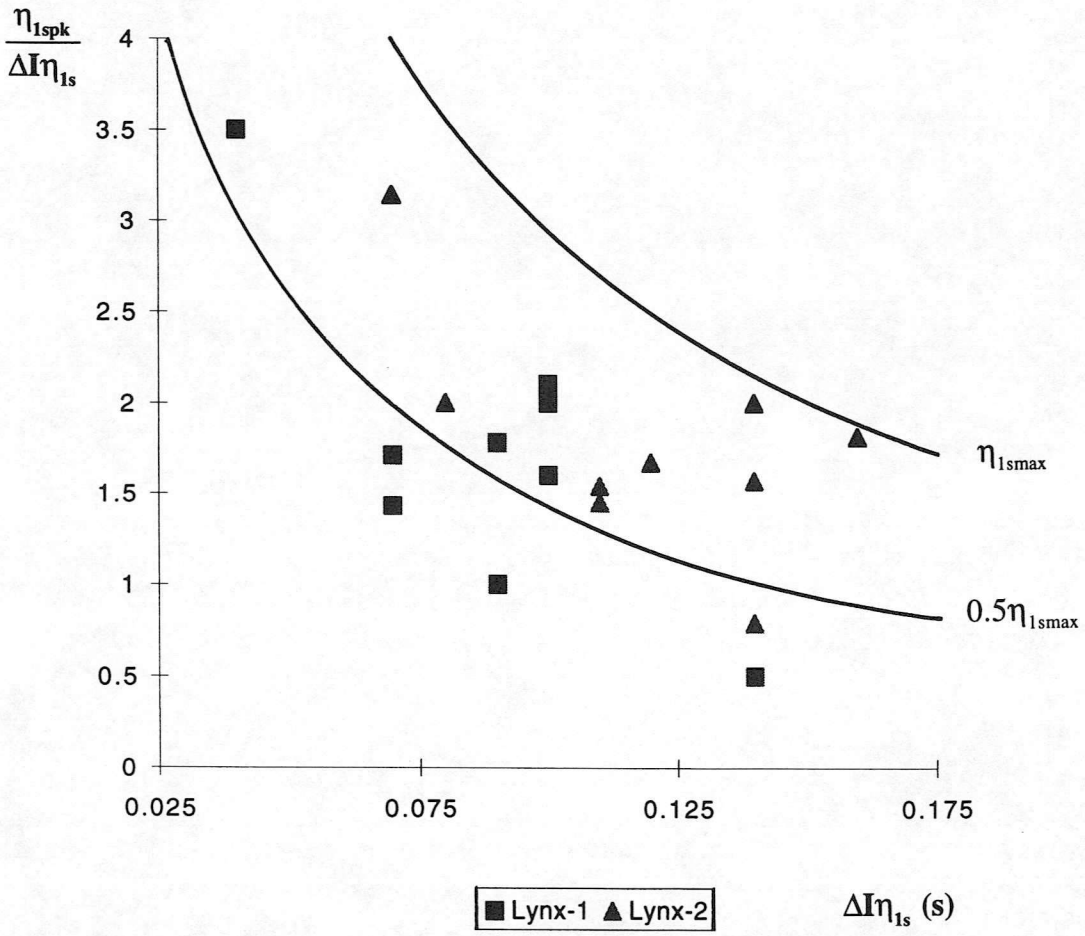

Figure 17 **Longitudinal cyclic stick displacement quickness chart for both Lynx configurations and all three rapid Quick-hop MTEs**

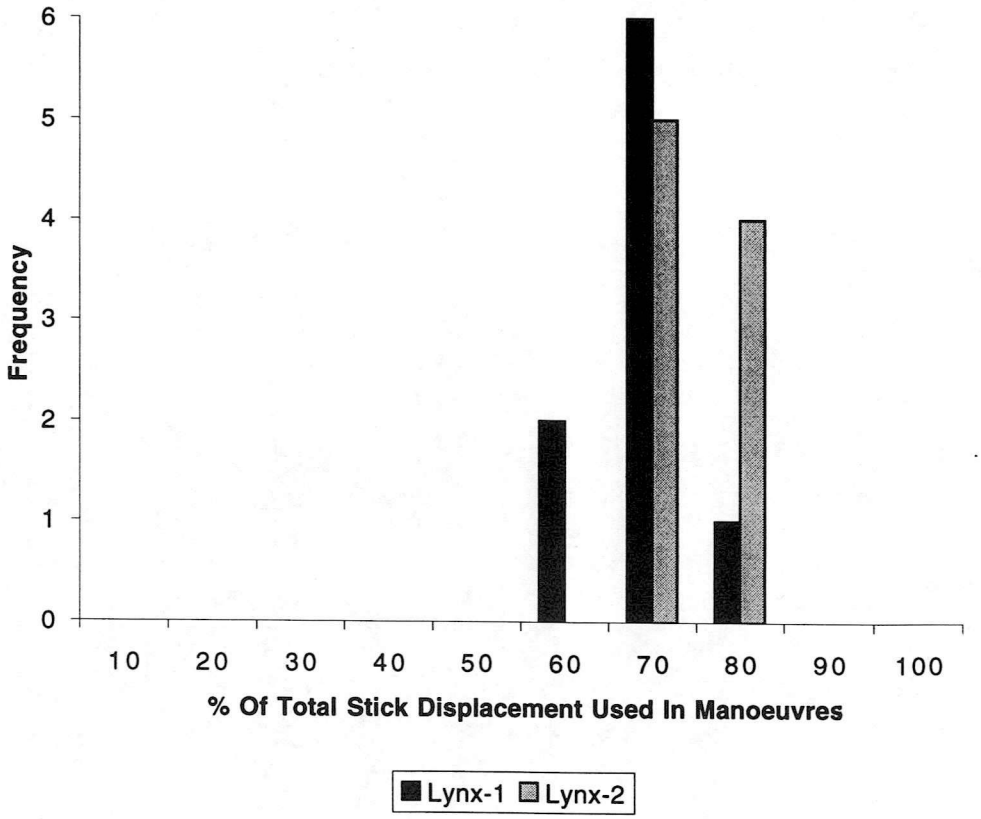

Figure 18 Longitudinal cyclic stick frequency chart

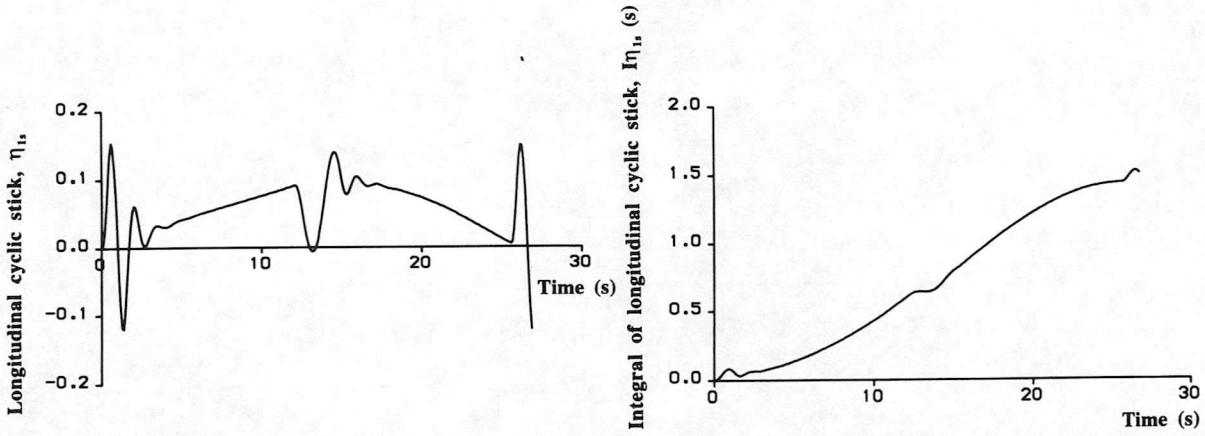

(a) Stability and Control Augmentation System (SCAS) Off

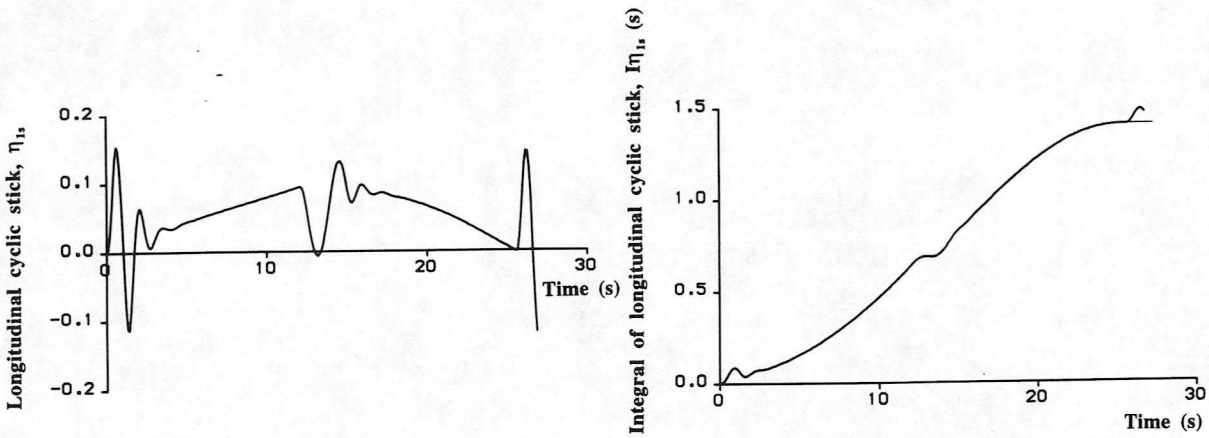

(b) Stability and Control Augmentation System (SCAS) On

Figure 19 Longitudinal cyclic stick displacement, η_{1s} and integral of longitudinal cyclic stick, $I\eta_{1s}$ time-histories for Lynx-1

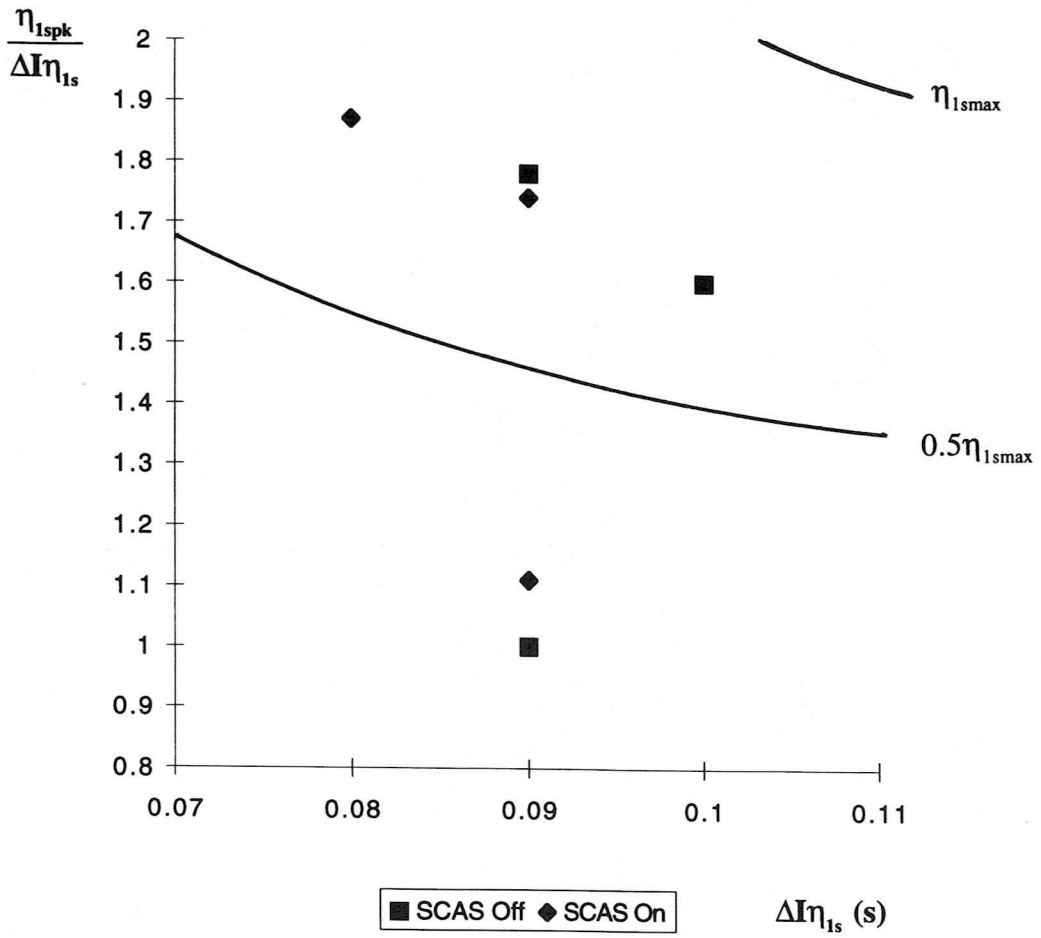

Figure 20 Longitudinal cyclic stick displacement quickness chart calculated from Figure 19 time-histories

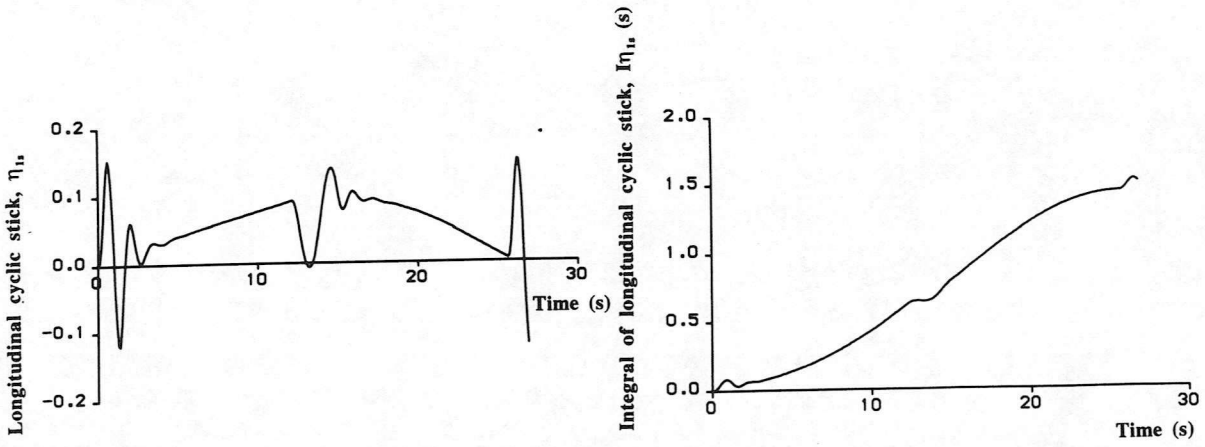

(a) Longitudinal cyclic actuator time constant, τ_{c1}=0.125 (normal)

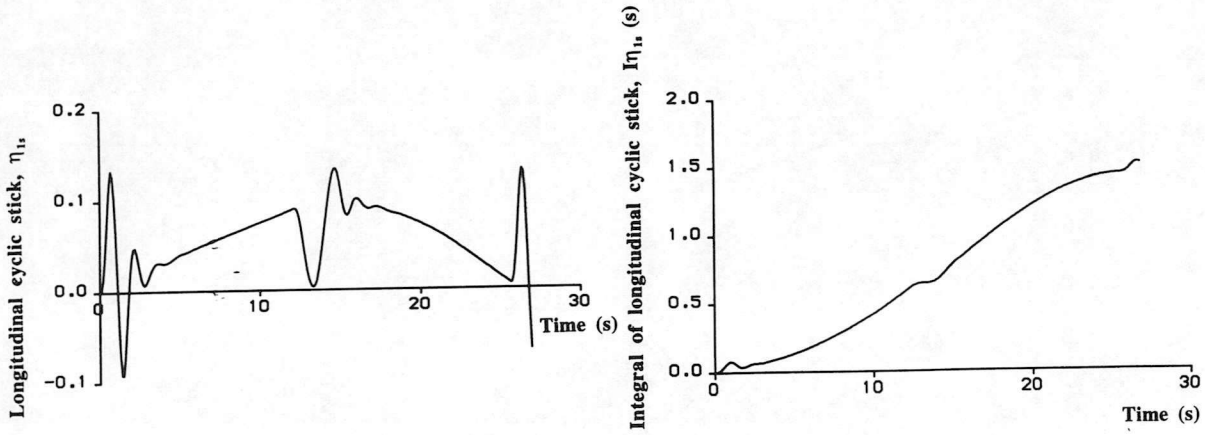

(b) Longitudinal cyclic actuator time constant, τ_{c1}=0.0

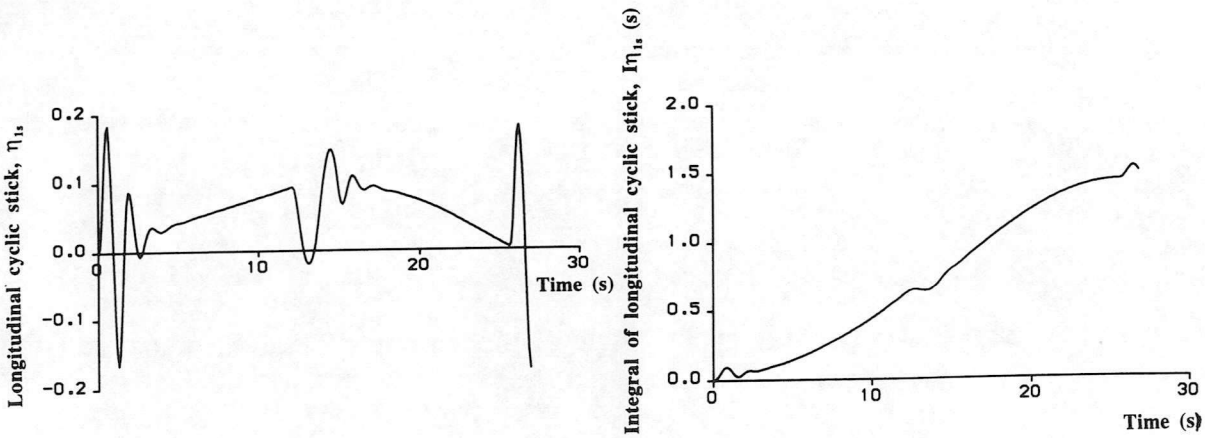

(c) Longitudinal cyclic actuator time constant, τ_{c1}=0.25

Figure 21 Longitudinal cyclic stick displacement, η_{1s} and integral of Longitudinal cyclic stick, $I\eta_{1s}$ time-histories for Lynx-1

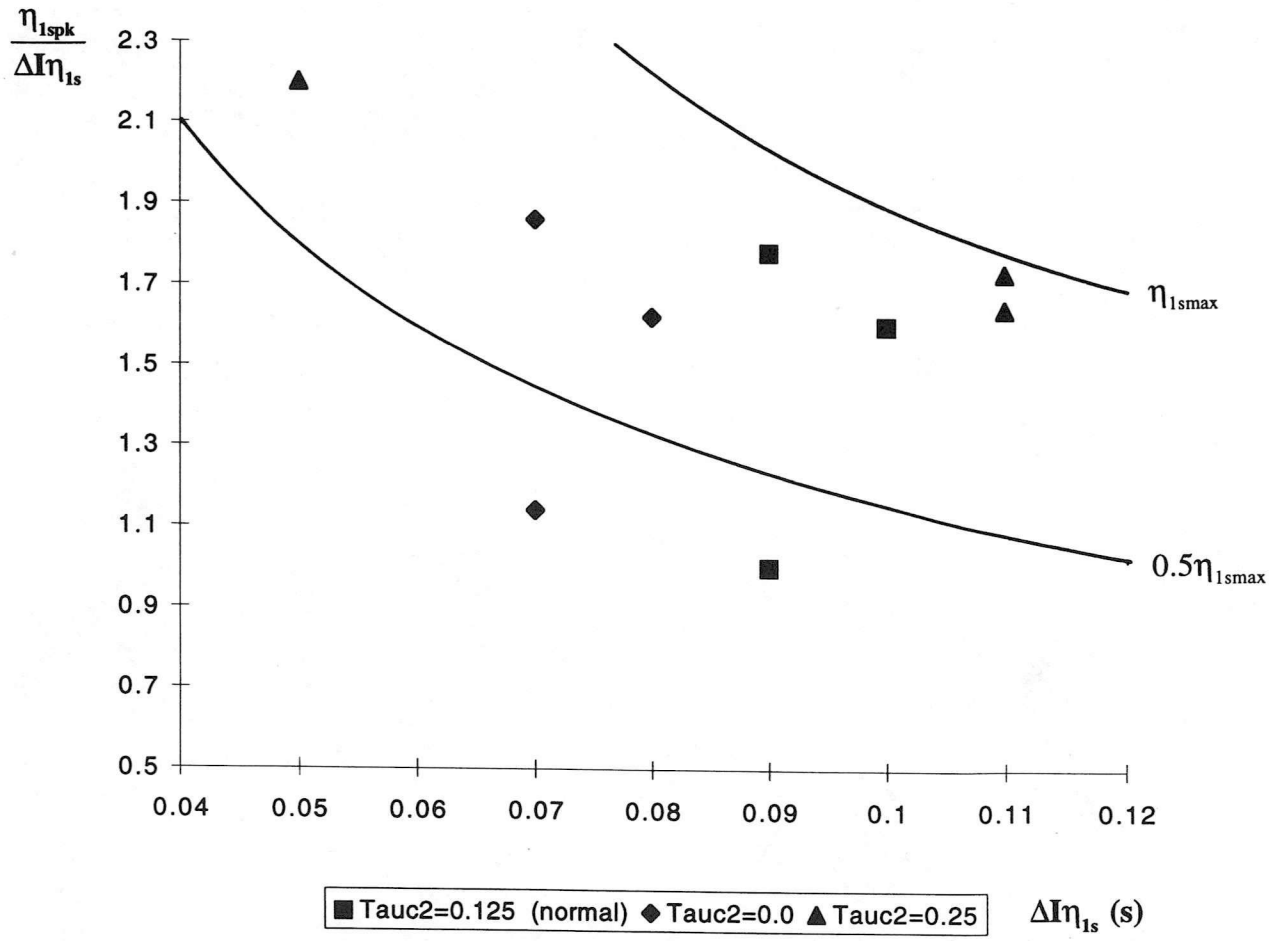

Figure 22 **Longitudinal cyclic stick displacement quickness chart calculated from Figure 21 time-histories**